Time-Dependent Structural Changes of the Dentatothalamic Pathway in Children Treated for Posterior Fossa Tumor

S. Perreault, R.M. Lober, S. Cheshier, S. Partap, M.S. Edwards, and K.W. Yeom

ABSTRACT

BACKGROUND AND PURPOSE: Injury to the dentatothalamic pathway that originates in the cerebellum has been suggested as a mechanism for neurologic complications in children treated for posterior fossa tumors. We hypothesized that time-dependent changes occur in the dentatothalamic pathway.

MATERIALS AND METHODS: Diffusion tensor evaluation was performed in 14 children (median age, 4.1 years; age range, 1–20 years) who underwent serial MR imaging at 3T as part of routine follow-up after posterior fossa tumor resection with or without adjuvant therapy. Tensor metrics were obtained in the acute (≤1 week), subacute (1 to <6 months), and chronic (≥6 months) periods after surgery. We evaluated the following dentatothalamic constituents: bilateral dentate nuclei, cerebellar white matter, and superior cerebellar peduncles. Serial dentate nuclei volumes were also obtained and compared with the patient's baseline.

RESULTS: The most significant tensor changes to the superior cerebellar peduncles and cerebellar white matter occurred in the subacute period, regardless of the tumor pathology or therapy regimen, with signs of recovery in the chronic period. However, chronic volume loss and reduced mean diffusivity were observed in the dentate nuclei and did not reverse. This atrophy was associated with radiation therapy and symptoms of ataxia.

CONCLUSIONS: Longitudinal diffusion MR imaging in children treated for posterior fossa tumors showed time-dependent tensor changes in components of the dentatothalamic pathway that suggest evolution of structural damage with inflammation and recovery of tissue directionality. However, the dentate nuclei did not show tensor or volumetric recovery, suggesting that the injury may be chronic.

ABBREVIATIONS: DTT = dentatothalamic; FA = fractional anisotropy; $\lambda_{\|}$ = perpendicular diffusivity; MD = mean diffusivity; PF = posterior fossa; PFS = posterior fossa syndrome; SCP = superior cerebellar peduncles; $\lambda_{\|}$ = parallel diffusivity

Posterior fossa (PF) tumors represent a significant number of pediatric brain tumors and largely comprise pilocytic astrocytoma, medulloblastoma, and ependymoma.[1] Despite an increase in survival from advances in therapy, many survivors of PF tumors have cognitive and various forms of cerebellar dysfunction thought to reflect brain injury incurred by a combination of tumor and treatment.[2-4] Given its important role not only in motor coordination but also in cognition, injuries to the cerebellum and, more specifically, the cerebrocerebellar pathway have been proposed as possible mechanisms.[5-7]

One such pathway, the dentatothalamic (DTT) tract, has been shown to display a role in linguistic and cognitive functions.[8-10] The DTT tract contains axons that originate in the dentate nucleus of the cerebellum, project through the ipsilateral superior cerebellar peduncle (SCP), decussate in the dorsal midbrain, and then terminate in the contralateral ventrolateral nucleus of the thalamus. From there, the axons project to the primary motor cortex as well as secondary and tertiary association areas within the frontal and parietal lobes.[11]

Studies have shown that injury to the DTT tract and associated degeneration may be implicated in cognitive and behavioral deficits as well as the development of posterior fossa syndrome (PFS), a unique constellation of symptoms including speech impairment, emotional lability, hypotonia, and ataxia.[12-15] Recent studies have used diffusion MR imaging to evaluate DTT pathways in patients treated for PF tumors but have reported variable DTI metric results.[12,13,16,17] A possible explanation might be that associated axonal degeneration, tissue inflammation, and repair that occur after injury are not static but evolve in a time-depen-

Received July 3, 2013; accepted after revision July 28.

From the Departments of Neurology (S. Perreault, S. Partap), Neurosurgery (R.M.L., S.C., M.S.E.), and Radiology (K.W.Y.), Lucile Packard Children's Hospital at Stanford, Palo Alto, California.

Please address correspondence to Kristen W. Yeom, MD, Department of Radiology, Lucile Packard Children's Hospital at Stanford, 725 Welch Rd, Room 0511A, Palo Alto, CA 94304; e-mail: kyeom@stanford.edu

Indicates article with supplemental on-line tables

http://dx.doi.org/10.3174/ajnr.A3735

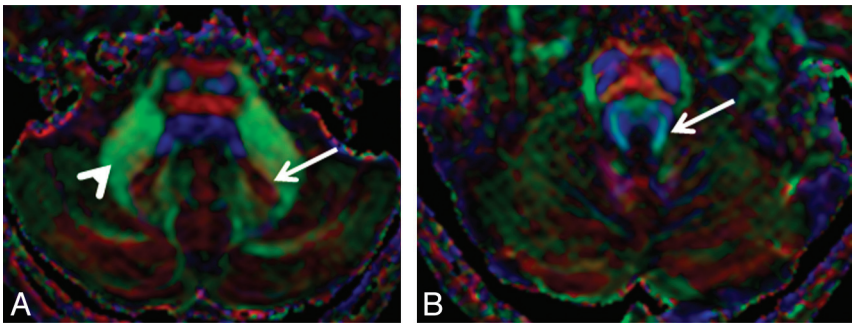

FIG 1. Eigenvector color maps. *A*, Long arrow indicates the dentate nucleus; arrowhead, the cerebellar white matter at the level of middle cerebellar peduncle. *B*, Long arrow indicates the superior cerebellar peduncle.

Clinical features of posterior fossa tumor patients

Patient Characteristics	No. (%)
Age at initial diagnosis (yr)	
Median	4.1
Range	1–20
Sex	
Male	9 (64)
Female	5 (36)
Diagnosis	
Medulloblastoma	7 (50)
Pilocytic astrocytoma	4 (29)
Ependymoma	2 (14)
Choroid plexus papilloma	1 (7)
Treatment modalities	
Surgery only	5 (36)
Surgery/chemotherapy	2 (14)
Surgery/chemotherapy/radiation therapy	7 (50)
Postoperative neurologic status	
Ataxia	8 (57)
Hemiplegia	5 (36)
No sequelae	5 (36)
Posterior fossa syndrome	3 (21)

dent manner.[18-20] A study that investigates temporally relevant tissue changes might provide insight into cerebellar injury and its evolution in children who undergo PF tumor therapy. We hypothesized that time-dependent changes occur in the DTT pathway as measured by DTI metrics and dentate nuclei volume in children treated for PF tumors.

MATERIALS AND METHODS

Subjects

All patients presenting with treatment-naïve PF tumor at our children's hospital between January 2010 and May 2012 were retrospectively reviewed after approval by the institutional review board (protocol 4223; No. 4947). The study cohort was identified by using the following inclusion criteria: The patient underwent DTI at 3T as part of routine tumor evaluation, subsequently underwent surgical resection of the tumor, and underwent a baseline DTI ≤1 week after surgery and follow-up DTI at least 1 month after surgery. Information regarding age at diagnosis, sex, tumor pathology, the presence of PFS or other neurologic complications, and postoperative clinical status at 1 month after surgery was collected. The time points for analysis after surgery were defined in the following manner: acute period (≤1 week after surgery), the subacute period (between 1 month and <6 months after surgery), and the chronic period (≥6 months after surgery).

Image Acquisition

A generalized autocalibrating partially parallel acquisition DTI was obtained at 3T MR imaging (Discovery 750; GE Healthcare, Milwaukee, Wisconsin) with an 8-channel head coil and a twice-refocused generalized autocalibrating parallel acquisitions diffusion tensor echo-planar imaging sequence (acquisition matrix = 128 ×128, acceleration factor = 3, NEX = 3, 25 isotropically distributed diffusion directions with b = 1000 s/mm^2, 5 b = 0 images, section thickness/gap = 3/0 mm, FOV = 20–24 cm) by using the reconstruction and motion-correction methods previously described.[21]

Imaging Analysis of DTT Pathway

Mean diffusivity (MD) and fractional anisotropy (FA) were obtained by using the region-of-interest analysis. These regions included the following: bilateral dentate nuclei, cerebellar white matter at the level of the middle cerebellar peduncle, and the SCP. One investigator (S. Perreault), blinded to clinical information, selected ROIs (Fig 1). Structures were first identified by using a combination of T1- and T2-weighted images and color eigenvector DTI maps and then were cross-referenced to the ADC (mean diffusivity) and FA maps. The ROIs were adjusted on the basis of the anatomy of each patient. For example, the ROIs for the SCP were ellipsoid and measured approximately 10 mm^2. The ROIs for the cerebellar white matter at the level of the middle cerebellar peduncle were circular and measured approximately 30 mm^2. Proper placement of the ROIs was confirmed independently by a blinded board-certified pediatric neuroradiologist (K.W.Y).

Bilateral dentate nuclei delineations conformed to their size and were performed by using the eigenvector color maps. Volume was measured by calculating the area within a region of interest multiplied by the 3-mm section thickness, similar to the method described by Du et al.[22]

Statistical Analyses

Statistical analyses were performed with the Statistical Package for the Social Sciences, Version 20.0 (IBM, Armonk, New York). Statistical analyses were conducted by using the Fisher exact test (2-tailed), Friedman 2-way analysis of variance by rank for related samples, and the Wilcoxon signed rank test for related samples. A general linear model was used to determine significant independent factors.

RESULTS

Patients with PF Tumor

Fourteen patients met the inclusion criteria and were included in the study. Median age at diagnosis was 4.1 years (age range, 1–20 years) (Table). Our patient cohort underwent 45 DTIs (median = 3 per patient; range, 2–4). The median time of DTI acquisition in the acute period was 3 days after surgery (range, 1–7 days); in the subacute period, 2.8 months after surgery (range, 1.2–5.8

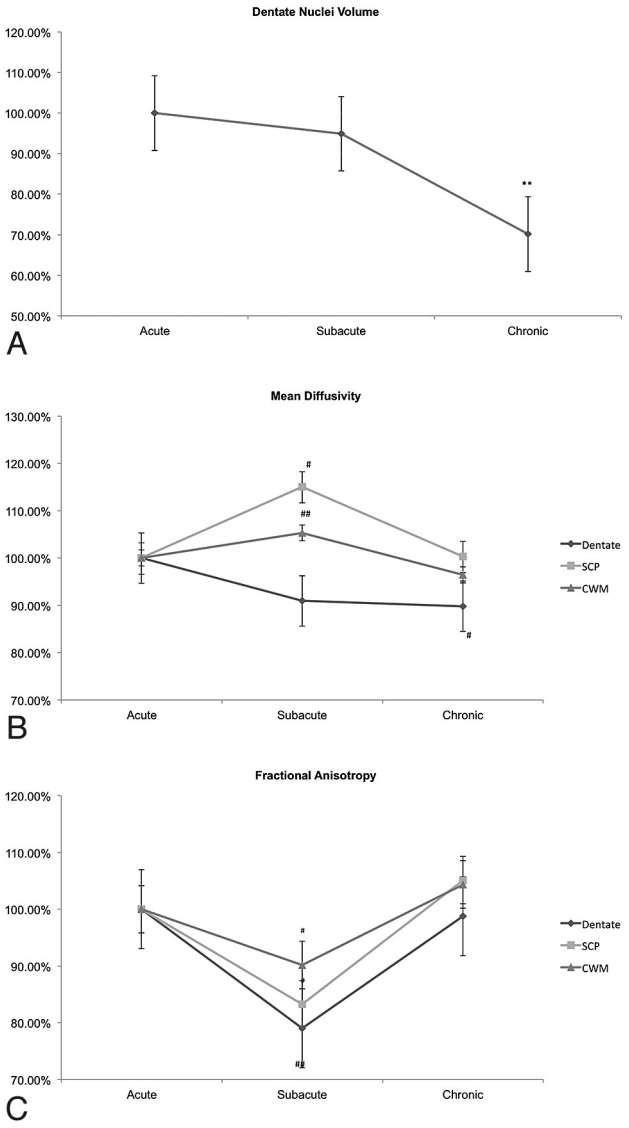

FIG 2. Mean variation from baseline of dentate nuclei volume, mean diffusivity, and fractional anisotropy during the acute, subacute, and chronic periods. *A*, Dentate nuclei volume variation. *B*, Mean diffusivity variation. *C*, Fractional anisotropy variation. CWM indicates cerebellar white matter. Error bars represent standard error of the mean. Double asterisks indicate Friedman 2-way analysis of variance by rank for related samples ($P < .01$); number sign, Wilcoxon signed rank test for related samples (double number sign, $P = .01$; number sign, $P \leq .05$).

months); and in the chronic period, 15.5 months after surgery (range, 6–29.4 months).

Medulloblastoma was the most frequent diagnosis with 7 patients (50%), followed by pilocytic astrocytoma ($n = 4$, 29%), ependymoma ($n = 2$, 14%), and choroid plexus papilloma ($n = 1$, 7%). No significant age difference was seen between medulloblastoma and other tumor groups (5.15 ± 3.2 versus 6.14 ±4.8 years, $P = .7$). Five patients (36%) underwent surgery only, 2 patients received chemotherapy after surgery (14%), and 7 patients (50%) received chemotherapy plus radiation therapy after initial tumor resection (Table). Three patients developed PFS in the postoperative period. One month after resection, 9 patients (64%) had either ataxia or hemiplegia and 5 patients had no sequelae.

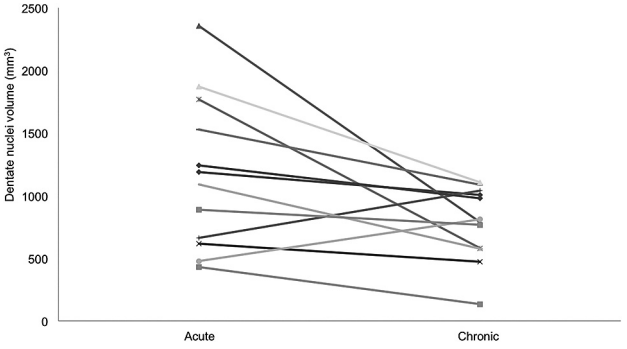

FIG 3. Combined dentate nuclei volume during the acute period compared with the chronic period for each patient.

Dentate Nuclei Volume

Among the patients with PF tumors, dentate nuclei volume remained stable in the acute and subacute periods but showed significant volume loss in the chronic period (389.3 mm^3 compared with 554.9 mm^3, $P = .007$) (Figs 2*A* and 3, On-line Table 1).

Mean Diffusivity

MD of the SCP increased and cerebellar white matter trended higher from the acute-to-subacute periods with a return close to postoperative baseline in the chronic time point (Fig 2*B*, On-line Table 1). The decrease in MD of the dentate nuclei was not significant between the acute and subacute periods but showed significant decrease in the chronic period (Fig 2*B*, On-line Table 1).

Fractional Anisotropy

The FA significantly decreased from the acute-to-subacute periods in the dentate nuclei and in the SCP but returned to the postoperative level during the chronic period. The FA of the cerebellar white matter trended lower from the acute-to-subacute periods and returned to the postoperative level during the chronic period (Fig 2*C*, On-line Table 1).

Tumor Group Differences

Tumor types, differences in treatment regimen, or neurologic sequelae were not associated with differences in MD or FA ($P > .3$).

All patients showed reduced total volume of the dentate nuclei except for 2 patients who had undergone surgery only for pilocytic astrocytomas and did not have any clinical sequelae. These patients with pilocytic astrocytoma did not have a significant change in dentate nuclei volume during the observation period (On-line Table 2). Factors associated with dentate nuclei atrophy were medulloblastoma, radiation therapy, presence of ataxia, and posterior fossa syndrome (On-line Table 2). With a general linear model, only radiation therapy and ataxia were related to atrophy of the dentate nuclei (partial eta squared, 0.22, $P = .03$ and .02, respectively). Tumor types and PFS did not contribute significantly to the model.

DISCUSSION

Our results showed that the most significant tensor changes to the SCP and cerebellar white matter occurred in the subacute period, or in the 1–6 months following PF tumor resection. Patients with PF tumors other than pilocytic astrocytoma showed significant volume loss and decrease in mean diffusivity of the dentate nuclei

in the chronic period. The presence of ataxia and prior radiation were positively associated with the presence of dentate nuclei atrophy. To our knowledge, this is the first study to examine longitudinal tensor and volumetric changes of the key components of the DTT pathway in children treated for PF tumors.

Prior studies have reported the sensitivity of diffusion MR imaging to axonal injury and have shown diffusion changes distal to the site of the lesion,[23-25] suggesting detection of Wallerian degeneration, which occurs when axons are separated from their cell body.[26] The DTT tract is the main outflow of the cerebellum, and it has been suggested that injury to the cerebellum and degeneration of this cerebrocerebellar pathway may be involved in cognitive dysfunction and PFS.[13,27-29] More recently, DTI metrics have shown tensor changes in the DTT pathway in patients treated for PF tumor, suggesting that DTI may be more robust than conventional MR imaging in probing structural damage.[12,13,16,30]

While prior studies have reported decreased FA of the SCP or increased MD of the cerebellar white matter in patients with PFS when examined at variable single-time points, our results show that the tensor changes may not be limited to those with symptoms of PFS.[13,16] In fact, when assessed longitudinally, all patients with treated PF tumors showed tensor changes at 1–6 months after surgery. These tensor changes (reduced FA and increased MD) showed significant improvement in the chronic period within both the SCP and the cerebellar white matter. Such tensor patterns suggest that tissue breakdown, inflammation, repair, or other injury-related features might be time-dependent. As previously described in animal models, axonal degeneration can occur as early as 30 minutes from the time of insult, with centrifugal disintegration and fragmentation of the axonal cytoskeleton and concomitant breakdown of the myelin sheaths.[18,20] Weeks later, inflammatory cells begin phagocytosis of the myelin and axon debris, a process that can last for many months.[18]

Reduced FA and increased MD may be explained by reduced axonal directionality and more uniform spatial water displacement that result from the breakdown of barriers that normally hinder water diffusion.[31,32] Studies have also shown that reduced FA or changes in MD can be attributed to a combination of reduced diffusivity parallel ($\lambda_{\parallel}$) to the principal axis of the fibers, which might arise from additional barriers imposed by axonal beading, bulges, fragmentation, and increased perpendicular diffusivity ($\lambda_{\perp}$), which might be seen with increased water mobility in perpendicular direction with myelin loss.[32-39]

Our study is consistent with a prior study by Concha et al,[40] which reported more significant tensor changes (lower FA and higher MD) at 2 months compared with 1 week after callosotomy in patients with epilepsy and similar time-dependent diffusion changes in the animal models of spinal injury.[23,41] In those studies, further assessment revealed decreased $\lambda_{\parallel}$ in the acute period (1 week) and elevated $\lambda_{\perp}$ at a later time (21 days to 2 months) after injury.[23,40,41] Given that $\lambda_{\parallel}$ may be more sensitive to axonal degeneration, whereas $\lambda_{\perp}$ changes may be driven by myelin effects, these studies suggested that varying contributions from axonal degeneration and myelin breakdown along different time points likely impacted temporal tensor differences, including both FA and MD.[23,40,41] Other studies have also suggested that an increase in $\lambda_{\perp}$ may drive the reduction in FA that occurs at a later time point in axonal degeneration.[42-44]

While individual FA and MD are not sufficient to differentiate axonal-versus-myelin degeneration, a pronounced reduction in FA and an increase in MD in the subacute period likely reflect the combined effects of active or ongoing myelin breakdown and inflammation after initial cerebellar injury.

Clinical factors associated with progressive decrease in dentate nuclei volume were radiation therapy, medulloblastoma (which often includes radiation as part of standard care), and symptoms of ataxia and PFS, whereas tensor changes occurred globally in all patients who underwent PF surgery. These findings suggest that the dentate nuclei may be particularly sensitive to the effects of radiation, with resultant injury and gliosis, as reflected by progressive volume loss and a decrease in MD. Symptoms of ataxia and PFS possibly reflect some aspect of dentate nuclei dysfunction. In comparison, tensor changes were seen in our general PF tumor cohort and may represent nonspecific sequelae of global cerebellar injury that combine tumor mass effect, edema, surgical manipulation, various therapy-induced excitotoxic events, inflammation, and local reactive tissue changes. This finding is also consistent with a prior report that did not find significant tensor differences among patients with PF tumor who underwent surgery only versus those who underwent surgery and radiation therapy.[12]

Given that an individual child's baseline myelination status, axonal density, and axonal diameter could influence diffusion metrics, each patient served as his or her own control in our longitudinal analysis. Although preoperative MR imaging might provide additional information, this was not feasible due to gross anatomic distortion by tumor, which would have rendered inaccurate measurements.

Despite certain limitations, this is the first study to demonstrate time-relevant structural changes that occur to the DTT pathway in children who have undergone therapy for PF tumors. Future studies that combine longitudinal DTT changes and cerebral connectivity could provide additional insight into treatment-related neurotoxicity and associated neurologic complications in children treated for PF tumors.

CONCLUSIONS

Longitudinal diffusion MR imaging in children treated for PF tumors showed time-dependent tensor changes in the components of the DTT pathway that suggest evolving structural damage, inflammation, and signs of tissue restoration and directionality. However, the dentate nuclei showed progressive atrophy and a decrease in MD in the chronic period. This volume loss was most significant in children treated with radiation therapy and symptoms of ataxia.

Disclosures: Sébastien Perreault—*UNRELATED*: *Grants/Grants Pending*: Fonds de la recherche en santé du Québec, *Comments*: fellowship grant.

REFERENCES

1. Arora RS, Alston RD, Eden TO, et al. **Age-incidence patterns of primary CNS tumors in children, adolescents, and adults in England.** *Neuro Oncol* 2009;11:403–13

2. Rønning C, Sundet K, Due-Tonnessen B, et al. **Persistent cognitive dysfunction secondary to cerebellar injury in patients treated for posterior fossa tumors in childhood.** *Pediatr Neurosurg* 2005; 41:15–21
3. Mabbott DJ, Penkman L, Witol A, et al. **Core neurocognitive functions in children treated for posterior fossa tumors.** *Neuropsychology* 2008;22:159–68
4. Spiegler BJ, Bouffet E, Greenberg ML, et al. **Change in neurocognitive functioning after treatment with cranial radiation in childhood.** *J Clin Oncol* 2004;22:706–13
5. Timmann D, Daum I. **Cerebellar contributions to cognitive functions: a progress report after two decades of research.** *Cerebellum* 2007;6:159–62
6. Kim SG, Ugurbil K, Strick PL. **Activation of a cerebellar output nucleus during cognitive processing.** *Science* 1994;265:949–51
7. Leiner HC, Leiner AL, Dow RS. **Cognitive and language functions of the human cerebellum.** *Trends Neurosci* 1993;16:444–47
8. Marx JJ, Iannetti GD, Thomke F, et al. **Topodiagnostic implications of hemiataxia: an MRI-based brainstem mapping analysis.** *Neuroimage* 2008;39:1625–32
9. Schmahmann JD, Sherman JC. **The cerebellar cognitive affective syndrome.** *Brain* 1998;121(pt 4):561–79
10. Müller RA, Chugani DC, Behen ME, et al. **Impairment of dentato-thalamo-cortical pathway in autistic men: language activation data from positron emission tomography.** *Neurosci Lett* 1998;245:1–4
11. Kwon HG, Hong JH, Hong CP, et al. **Dentatorubrothalamic tract in human brain: diffusion tensor tractography study.** *Neuroradiology* 2011;53:787–91
12. Law N, Bouffet E, Laughlin S, et al. **Cerebello-thalamo-cerebral connections in pediatric brain tumor patients: impact on working memory.** *Neuroimage* 2011;56:2238–48
13. Morris EB, Phillips NS, Laningham FH, et al. **Proximal dentato-thalamocortical tract involvement in posterior fossa syndrome.** *Brain* 2009;132:3087–95
14. Robertson PL, Muraszko KM, Holmes EJ, et al. **Incidence and severity of postoperative cerebellar mutism syndrome in children with medulloblastoma: a prospective study by the Children's Oncology Group.** *J Neurosurg* 2006;105:444–51
15. Huber JF, Bradley K, Spiegler BJ, et al. **Long-term effects of transient cerebellar mutism after cerebellar astrocytoma or medulloblastoma tumor resection in childhood.** *Childs Nerv Syst* 2006;22:132–38
16. Law N, Greenberg M, Bouffet E, et al. **Clinical and neuroanatomical predictors of cerebellar mutism syndrome.** *Neuro Oncol* 2012;14: 1294–303
17. Lober RM, Perreault S, Partap S, et al. **Injury to dentate nuclei and efferent fibers by pediatric posterior fossa tumors.** *Neuro Oncol* 2012;14(suppl 1):132
18. George R, Griffin JW. **The proximo-distal spread of axonal degeneration in the dorsal columns of the rat.** *J Neurocytol* 1994;23:657–67
19. George R, Griffin JW. **Delayed macrophage responses and myelin clearance during Wallerian degeneration in the central nervous system: the dorsal radiculotomy model.** *Exp Neurol* 1994;129: 225–36
20. Kerschensteiner M, Schwab ME, Lichtman JW, et al. **In vivo imaging of axonal degeneration and regeneration in the injured spinal cord.** *Nat Med* 2005;11:572–77
21. Skare S, Newbould RD, Clayton DB, et al. **Clinical multishot DW-EPI through parallel imaging with considerations of susceptibility, motion, and noise.** *Magn Reson Med* 2007;57:881–90
22. Du AX, Cuzzocreo JL, Landman BA, et al. **Diffusion tensor imaging reveals disease-specific deep cerebellar nuclear changes in cerebellar degeneration.** *J Neurol* 2010;257:1406–08
23. Cohen-Adad J, Leblond H, Delivet-Mongrain H, et al. **Wallerian degeneration after spinal cord lesions in cats detected with diffusion tensor imaging.** *Neuroimage* 2011;57:1068–76
24. Cohen-Adad J, Benali H, Hoge RD, et al. **In vivo DTI of the healthy and injured cat spinal cord at high spatial and angular resolution.** *Neuroimage* 2008;40:685–97
25. DeBoy CA, Zhang J, Dike S, et al. **High-resolution diffusion tensor imaging of axonal damage in focal inflammatory and demyelinating lesions in rat spinal cord.** *Brain* 2007;130:2199–210
26. Beirowski B, Adalbert R, Wagner D, et al. **The progressive nature of Wallerian degeneration in wild-type and slow Wallerian degeneration (WldS) nerves.** *BMC Neurosci* 2005;6:6
27. McMillan HJ, Keene DL, Matzinger MA, et al. **Brainstem compression: a predictor of postoperative cerebellar mutism.** *Childs Nerv Syst* 2009;25:677–81
28. Ogiwara H, Dipatri AJ Jr, Bowman RM, et al. **Diffuse postoperative cerebellar swelling in medulloblastoma: report of two cases.** *Childs Nerv Syst* 2011;27:743–47
29. Rao VK, Haridas A, Nguyen TT, et al. **Symptomatic cerebral vasospasm following resection of a medulloblastoma in a child.** *Neurocrit Care* 2013;18:84–88
30. Beaulieu C. **The basis of anisotropic water diffusion in the nervous system: a technical review.** *NMR Biomed* 2002;15:435–55
31. Beaulieu C, Does MD, Snyder RE, et al. **Changes in water diffusion due to Wallerian degeneration in peripheral nerve.** *Magn Reson Med* 1996;36:627–31
32. Song SK, Yoshino J, Le TQ, et al. **Demyelination increases radial diffusivity in corpus callosum of mouse brain.** *Neuroimage* 2005;26:132–40
33. Ochs S, Pourmand R, Jersild RA Jr, et al. **The origin and nature of beading: a reversible transformation of the shape of nerve fibers.** *Prog Neurobiol* 1997;52:391–426
34. Budde MD, Kim JH, Liang HF, et al. **Axonal injury detected by in vivo diffusion tensor imaging correlates with neurological disability in a mouse model of multiple sclerosis.** *NMR Biomed* 2008; 21:589–97
35. Budde MD, Xie M, Cross AH, et al. **Axial diffusivity is the primary correlate of axonal injury in the experimental autoimmune encephalomyelitis spinal cord: a quantitative pixelwise analysis.** *J Neurosci* 2009;29:2805–13
36. Kim JH, Loy DN, Liang HF, et al. **Noninvasive diffusion tensor imaging of evolving white matter pathology in a mouse model of acute spinal cord injury.** *Magn Reson Med* 2007;58:253–60
37. Mac Donald CL, Dikranian K, Bayly P, et al. **Diffusion tensor imaging reliably detects experimental traumatic axonal injury and indicates approximate time of injury.** *J Neurosci* 2007;27:11869–76
38. Song SK, Sun SW, Ramsbottom MJ, et al. **Dysmyelination revealed through MRI as increased radial (but unchanged axial) diffusion of water.** *Neuroimage* 2002;17:1429–36
39. Zhang J, Jones M, DeBoy CA, et al. **Diffusion tensor magnetic resonance imaging of Wallerian degeneration in rat spinal cord after dorsal root axotomy.** *J Neurosci* 2009;29:3160–71
40. Concha L, Gross DW, Wheatley BM, et al. **Diffusion tensor imaging of time-dependent axonal and myelin degradation after corpus callosotomy in epilepsy patients.** *Neuroimage* 2006;32:1090–99
41. Farrell JA, Zhang J, Jones MV, et al. **Q-space and conventional diffusion imaging of axon and myelin damage in the rat spinal cord after axotomy.** *Magn Reson Med* 2010;63:1323–35
42. Wieshmann UC, Symms MR, Clark CA, et al. **Wallerian degeneration in the optic radiation after temporal lobectomy demonstrated in vivo with diffusion tensor imaging.** *Epilepsia* 1999;40:1155–58
43. Werring DJ, Toosy AT, Clark CA, et al. **Diffusion tensor imaging can detect and quantify corticospinal tract degeneration after stroke.** *J Neurol Neurosurg Psychiatry* 2000;69:269–72
44. Thomalla G, Glauche V, Weiller C, et al. **Time course of Wallerian degeneration after ischaemic stroke revealed by diffusion tensor imaging.** *J Neurol Neurosurg Psychiatry* 2005;76:266–68